Supporting Information

Failure of multi-layer graphene coatings in acidic media

*Feng Yu, Adam C. Stoot, P. Bøggild, Luca Camilli**

Technical University of Denmark, Department of Micro- and Nanotechnology, Kgs. Lyngby, DK-2800, Denmark

**email:* lcam@nanotech.dtu.dk

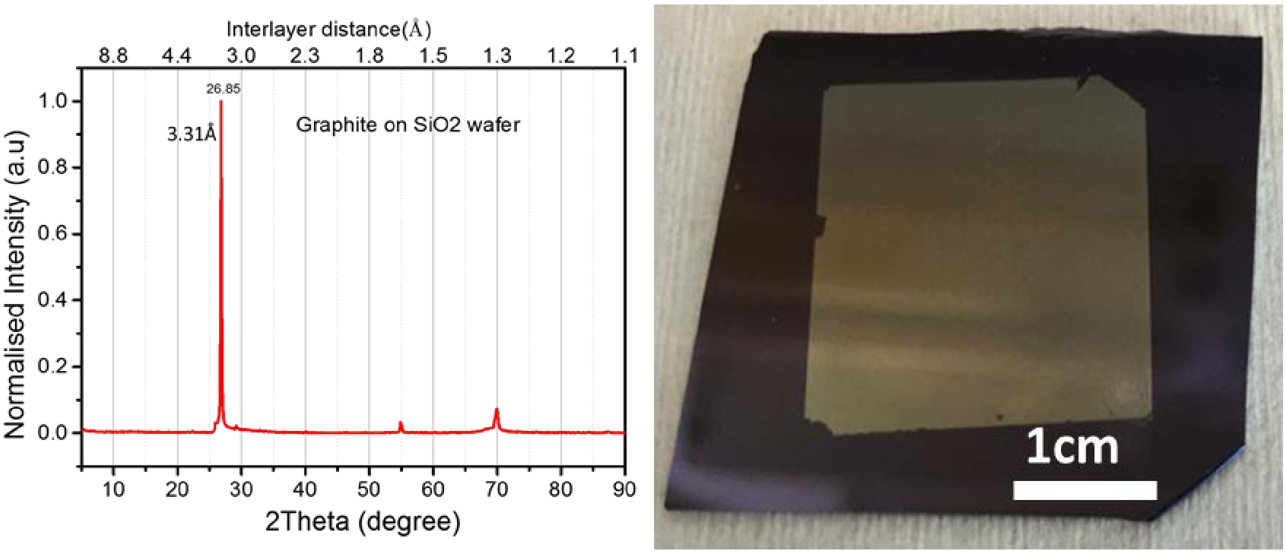

Figure S1. (left) X-ray diffraction pattern (CuKα excitation source) of a multilayer graphene (MLG) film deposited on a ~88nm SiO_2 substrate (right). The main peak, at around 27 degree, is due to the diffraction from the (002) planes of the graphitic film and gives an average interlayer distance of 3.31Å.

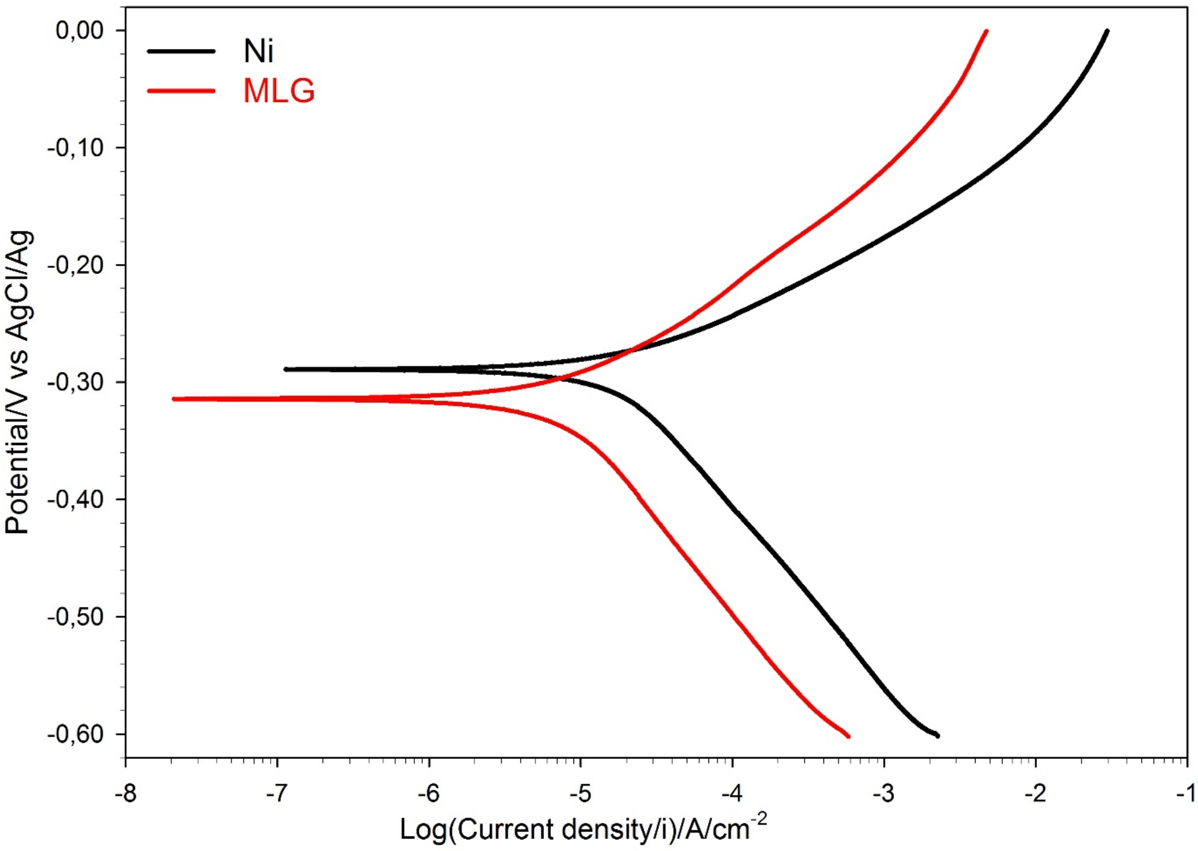

Figure S2. Polarization scans of both bare (dark curve) and MLG-coated (red curve) Ni samples after immersion in 0.5M HCl for 1 hour. The intersect between the extrapolation of the linear regions on both the cathodic and the anodic side of the current density minimum gives the corrosion potential (-290mV for bare nickel, -315mV for MLG-coated nickel) along with the corrosion current, I_{corr} (21µA/cm^2 and 9µA/cm^2 for bare and MLG-coated nickel, respectively). This, in turn, can be used to estimate the corrosion rate of the two systems: $CR = \frac{I_{corr} \cdot K \cdot EW}{\rho \cdot A}$ wherein K = 3272 mm/year, Nickel equivalent weight (EW) = 29g and the area is the expose working electrode area (A)[1]. The corrosion rates are calculated to be 0.226mm/year for bare nickel and 0.097mm/year for MLG-coated nickel.

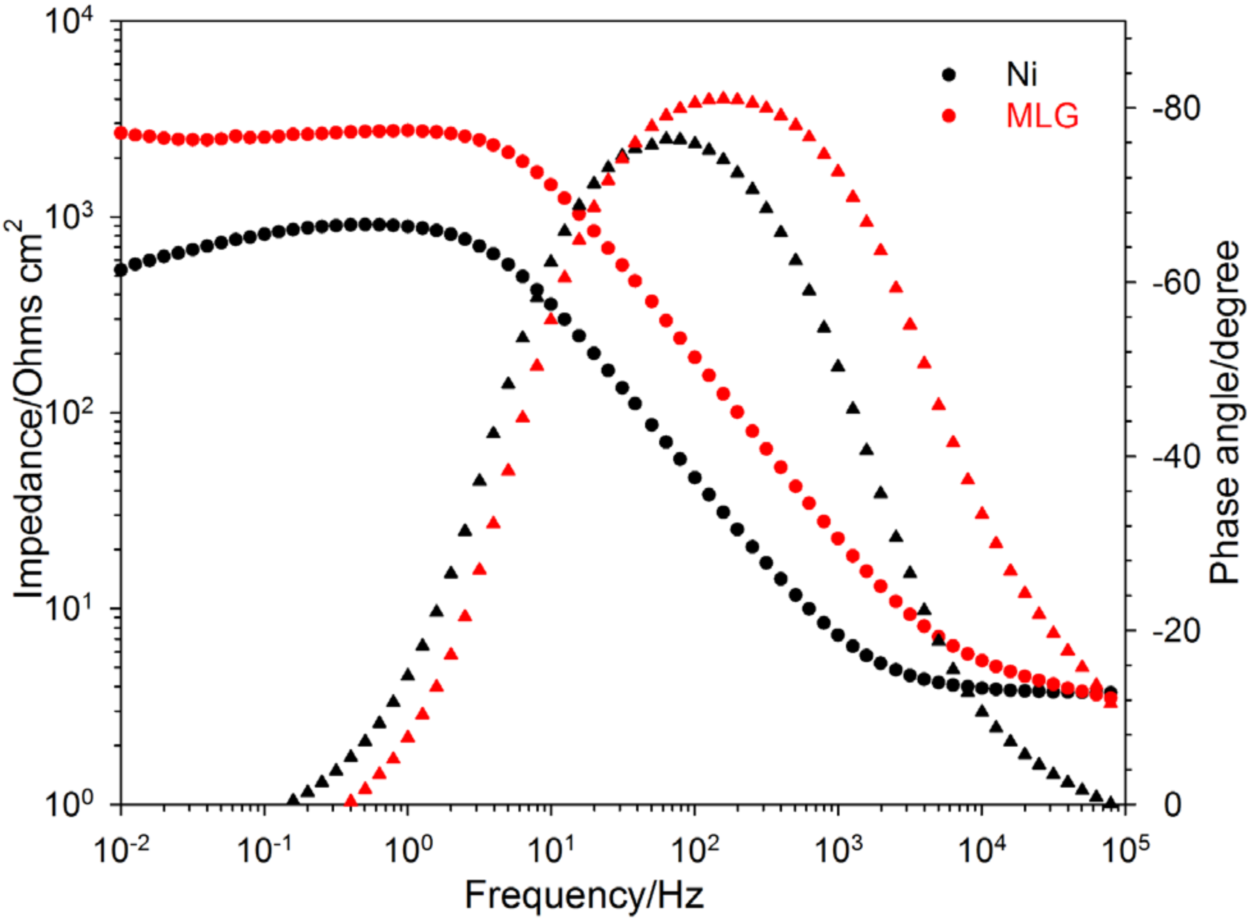

Figure S3. Electrochemical impedance spectroscopy of both Ni (black curves) and MLG-coated Ni (red curves) after immersion in 0.5M HCl for 1 hour. The magnitude of impedance (circles) at 10mHz for MLG-coated Ni samples is ~2700 Ω·cm^2, which is 5 times the value of ~540 Ω·cm^2 for bare Ni. This further indicates that MLG-coated Ni is more corrosion resistant than bare Ni. In the case of MLG-coated Ni, in the medium frequency region (10-1000Hz), both a shift to higher values of impedance (circles) and a shift to higher frequencies of time constant (triangles) can be observed when compared with bare Ni (with the time constant being the frequency where phase angle reaches the highest value on phase diagram). These features suggest that the double layer capacitance on MLG-coated Ni is lower than that of bare Ni, indicating that, to some extent, the MLG coating is acting as a barrier.

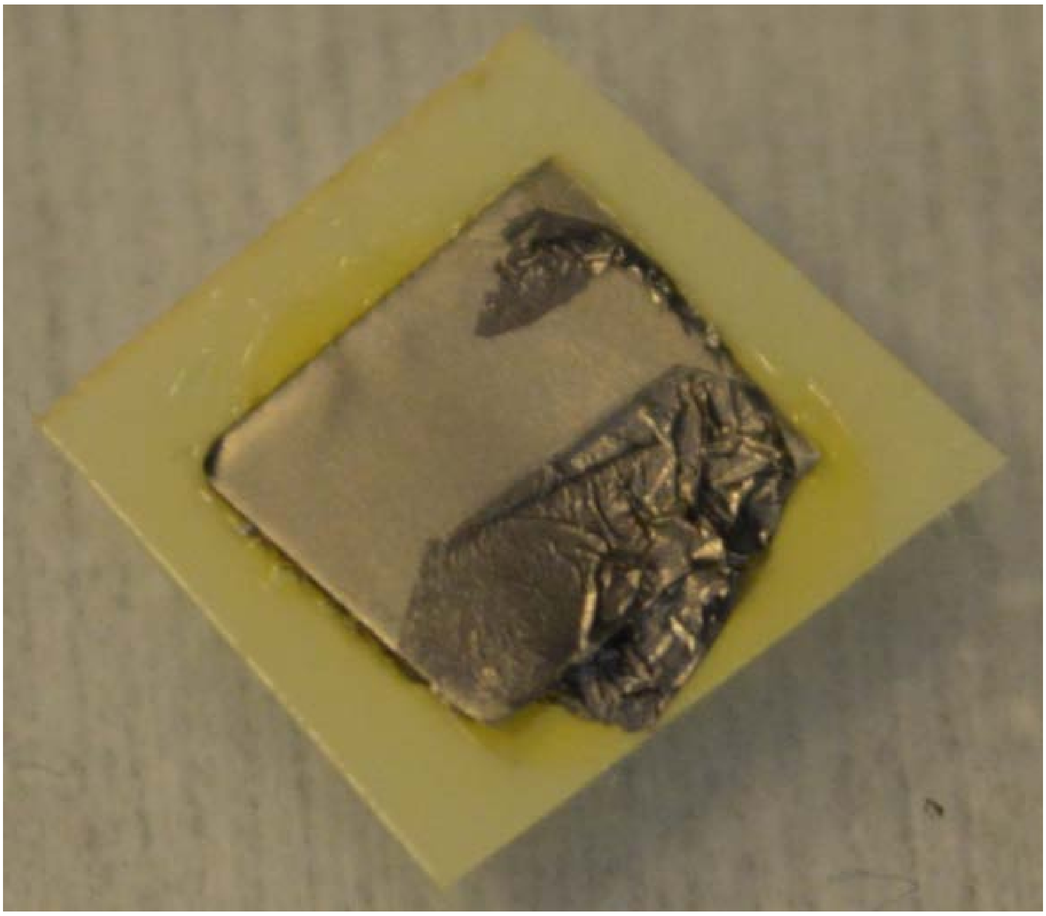

Figure S4. Delamination of the MLG coating from nickel substrate. A drop of 0.5M HCl solution was placed on a MLG-coated Ni sample, covering the whole surface. After 18 hours, the acid was removed by carefully absorbing it with a tissue, without touching the MLG coating. As can be seen from the picture, nearly the whole MLG film was delaminated from the nickel substrate due to the hydrogen bubbles formed at the MLG and Ni interface, with subsequent loss of adhesion of the coating.

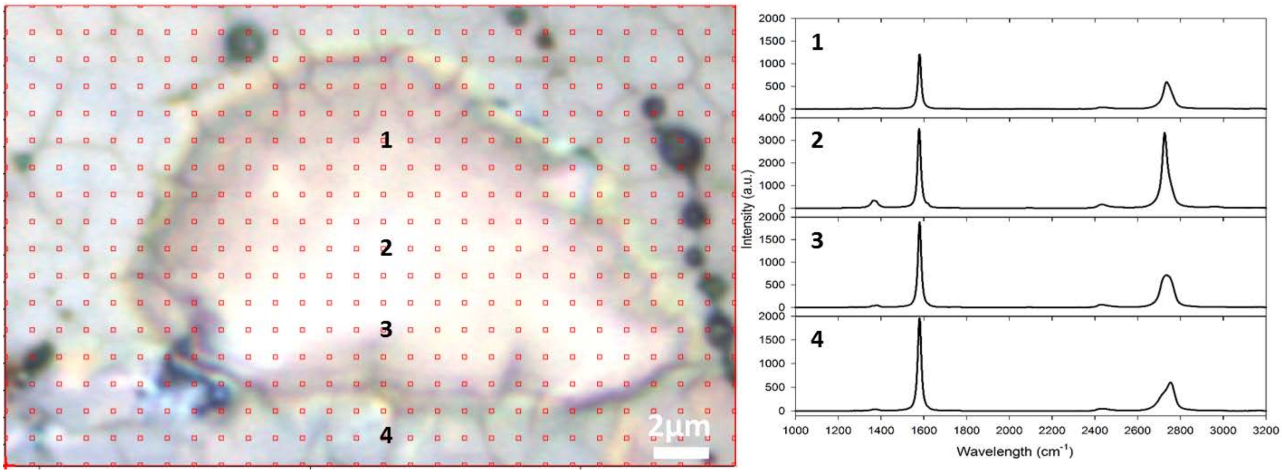

Figure S5. (left) Optical image and (right) Raman spectra of a blister formed under the MLG film. MLG-coated Ni sample was immersed in 0.5M HCl with an applied potential of -0.6V (vs. AgCl/Ag reference electrode) for 3min. Then, one of the blisters, which were found at the interface between MLG coating and nickel substrate, was analysed by Raman spectroscopy. The Raman spectra taken at different spots on top of the blister (point 1, 2 and 3) and outside (point 4) indicate the absence of any remarkable shift in the graphene peaks.

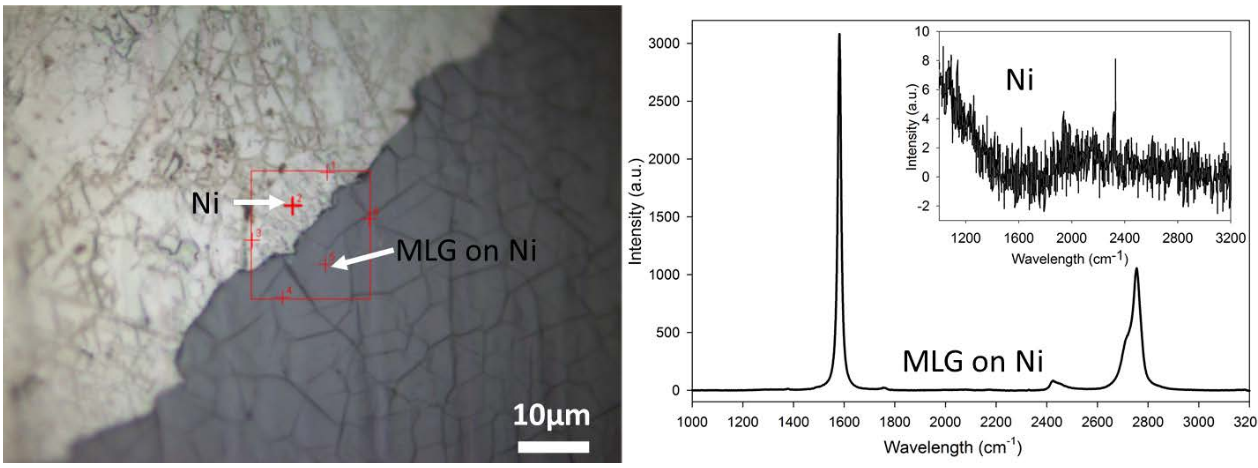

Figure S6. (left) Optical image and (right) Raman spectra of an area of the coated nickel sample where the MLG coating was partially delaminated. MLG-coated Ni sample was immersed in 0.5M HCl with an applied potential of -0.6V (vs. AgCl/Ag reference electrode) for 30min. The MLG coating was thus locally delaminated, showing some areas with no coating (left). The absence of the coating in this area is also proved by Raman spectroscopy (right).

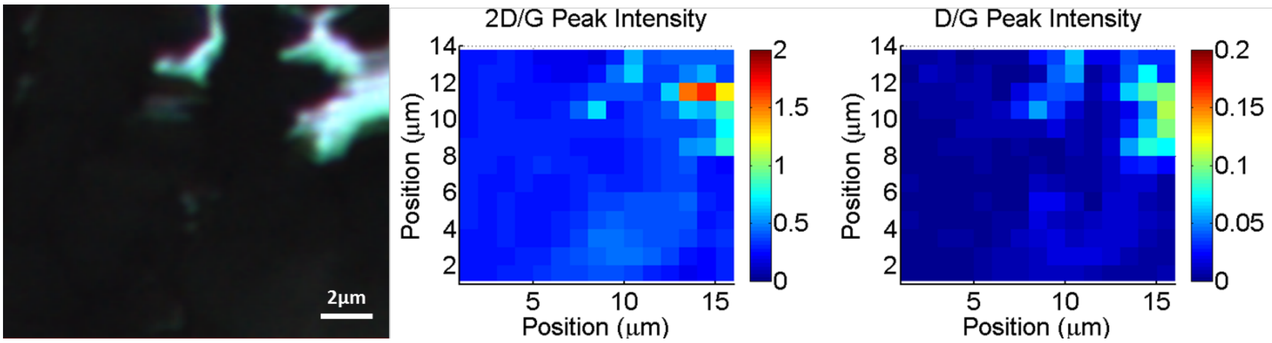

Figure S7. Optical image (left) with back illumination and relative Raman map (2D/G, at centre, and D/G, at right) of a transferred MLG film on a glass slide. The MLG is transferred on a glass slide and placed inside the Raman microscope. Back illumination is used to pinpoint the location of inhomogeneities in the MLG film (displayed as bright spots in the optical image at left). Raman map is then used to investigate the MLG film. The bright features found in the optical images show a higher defect density (see the D/G map, right panel) and a fewer number of layers (see 2D/G map, centre panel) with respect to the rest of the MLG film. These inhomogeneities are thought to be weak points in the coating and during the electrochemical tests they create paths for the acid, which can reach the nickel surface thus producing hydrogen.

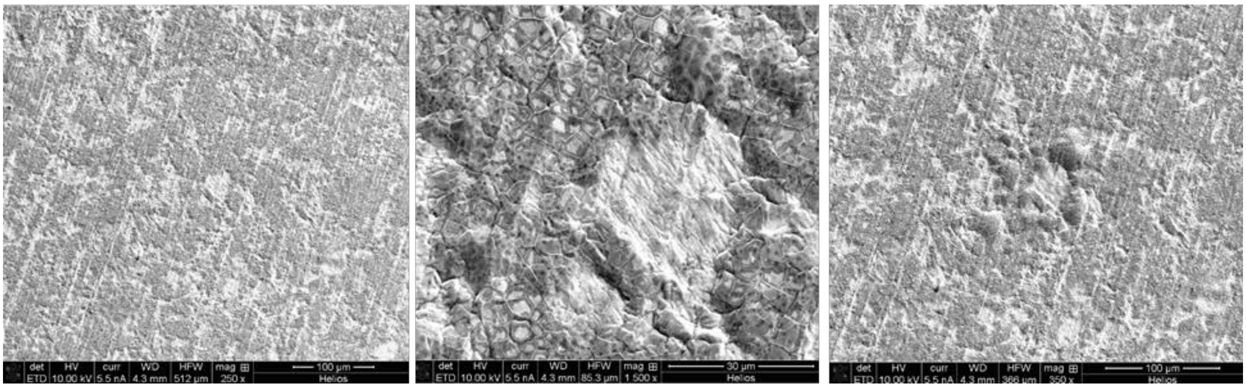

Figure S8. *In-situ* evolution of hydrogen in SEM. A droplet of 0.5 M HCl solution is placed in the centre of a MLG-coated nickel foil, and gently removed with a tissue. The sample is then mounted inside a SEM without prior rinsing or blow-drying. When the electron beam is focused on a flat region of the sample (left panel), some hydrogen bubbles are generated under the MLG coating (centre panel). At lower magnification, it is possible to see that the blister-like protrusions in the coating are mainly found in the area that was initially irradiated by the scanning electron beam (right panel).

References

1. Cottis, R. Shreir's Corrosion. Elsevier Amsterdam: 2010